Available online at www.sciencedirect.com
ScienceDirect
Journal of Solid State Chemistry 180 (2007) 1236–1242
JOURNAL OF SOLID STATE CHEMISTRY
www.elsevier.com/locate/jssc

Syntheses of rare-earth metal oxide nanotubes by the sol–gel method assisted with porous anodic aluminum oxide templates

Qin Kuang, Zhi-Wei Lin, Wei Lian, Zhi-Yuan Jiang, Zhao-Xiong Xie*, Rong-Bin Huang, Lan-Sun Zheng

Department of Chemistry, State Key Laboratory for Physical Chemistry of Solid Surfaces, College of Chemistry and Chemical Engineering, Xiamen University, Xiamen 361005, China

Received 18 November 2006; received in revised form 9 January 2007; accepted 22 January 2007
Available online 2 February 2007

Abstract

In this paper, we report a versatile synthetic method of ordered rare-earth metal (RE) oxide nanotubes. RE (RE = Y, Ce, Pr, Nd, Sm, Eu, Gd, Tb, Dy, Ho, Er, Yb) oxide nanotubes were successfully prepared from corresponding RE nitrate solution via the sol–gel method assisted with porous anodic aluminum oxide (AAO) templates. Scanning electron microscopy (SEM), transmission electron microscopy (TEM), high-resolution TEM, and X-ray diffraction (XRD) have been employed to characterize the morphology and composition of the as-prepared nanotubes. It is found that as-prepared RE oxides evolve into bamboo-like nanotubes and entirely hollow nanotubes. A new possible formation mechanism of RE oxide nanotubes in the AAO channels is proposed. These high-quantity RE oxide nanotubes are expected to have promising applications in many areas such as luminescent materials, catalysts, magnets, etc.

Keywords: Nanotube; Rare-earth metal oxide; AAO template; Sol–gel

1. Introduction

As conventional functional materials, rare-earth (RE) compounds (hydroxides, oxides, oxysulfides, fluoride, etc.) have been widely used in various fields in the past decades, such as high-performance luminescent devices, magnets and catalysts [1–3]. Popularity of these RE compounds in the application mainly originates from their special optical, electronic and magnetic properties that result from the electrons of the 4*f* shell. Recently, the potential improvement of material performance as a result of shape-specific and quantum-confinement further stimulates increasing research interests in low-dimensional RE compound nanostructures, especially in one-dimensional nanostructures such as nanowires, and nanotubes [4–6]. For example, Yada et al. [7,8] firstly synthesized RE (Er, Tm, Yb, Lu) oxide nanotubes templated by dodecylsulfate assemblies by the homogeneous precipitation method using urea. After that, Xu and co-workers prepared large-scale $Tb(OH)_3$, Tb_4O_7, $Y(OH)_3$ and Y_2O_3 nanotubes via a hydrothermal treatment of the corresponding bulk crystals and subsequent calcination treatment [9]. Li and co-workers further achieved the syntheses of RE compounds (including hydroxide and oxides) nanowires, nanotubes and fullerene-like nanoparticles by means of a facile hydrothermal synthetic pathway [10–12]. These soft-template or template-free strategies are powerful for the preparation of large amount of RE compound nanostructures. However, these strategies are difficult to be applied to prepare the order array structures that are sometimes very important in many important technical applications like laser emitter and display [13,14]. Therefore, it still requires continuous effort to explore some efficient and versatile synthetic methods to obtain high-yield and ordered RE compounds nanostructures.

Porous anodic aluminum oxide (AAO) membrane, a well-known hard template, plays an important role in the preparation of well-arranged one-dimensional nanostructures [15–18]. Meanwhile, the sol–gel method based on the

*Corresponding author. Fax: +86 592 2183047.
E-mail address: zxxie@xmu.edu.cn (Z.-X. Xie).

0022-4596/$ - see front matter © 2007 Published by Elsevier Inc.
doi:10.1016/j.jssc.2007.01.021

hydrolysis and condensation of precursor solution has many unique advantages in the preparation of multi-component nanomaterials [19]. Its biggest advantage is that the constituent materials can be easily homogeneously mixed at the molecular level by means of properly controlling the hydrolysis and condensation process. When combining homogeneous precipitation of the sol–gel method with the high order of AAO template, a great combinatorial advantage breaks a new path for the versatile syntheses of one-dimensional ordered multicomponent nanowires/nanotubes [20–26]. Inspired by this idea, we recently synthesized high-yield Eu-doped and undoped ThO_2 nanotubes from its nitrate solution by means of the sol–gel method assisted with porous AAO templates [27]. By keeping the well shape of nanotubes, the RE element Eu can be homogeneously doped into the ThO_2 crystal lattice in the wide doping range. In this paper, we report a versatile synthetic method of ordered RE oxide nanotubes. A series of RE oxide nanotube arrays (RE = Y, Ce, Pr, Nd, Sm, Eu, Gd, Tb, Dy, Ho, Er, Yb) were successfully prepared from corresponding RE nitrate solution via the sol–gel method assisted with porous AAO templates.

2. Experimental

2.1. Synthesis of porous AAO templates

The AAO templates were prepared using a one-step anodizing process as reported in our previous papers [27,28]. After preparation of the porous AAO film, the pores of AAO were widened to about 80 nm by dipping the AAO film into 5% phosphoric acid solution for half an hour at room temperature. Then, the AAO template was rinsed with distilled water and kept in a desiccator under low pressure for more than 8 h in order to drive out the gases trapped inside the pores. The pore depth of the AAO templates was about 20 μm.

2.2. Synthesis of ordered RE oxide nanotubes

In our experiments, we selected 12 RE (RE = Y, Ce, Pr, Nd, Sm, Eu, Gd, Tb, Dy, Ho, Er, Yb) oxides as typical examples. In a typical experiment, 0.5 g RE oxides were dissolved by adding nitric acid (60 wt%) in 50 mL distilled water and the resulting mixture was stirred in a water bath of 100 °C till white sols was formed. The pH value of the resulting sols is about 2–3. The AAO templates were immersed into the sols for 2 h under relative vacuum ambience. Then, the AAO templates were placed in a furnace and heated to a desired temperature (500 °C) within 20 min. After being annealed at 500 °C for 2 h, the AAO templates were cooled down to room temperature naturally. Excess products on the AAO surfaces were carefully wiped off.

2.3. Characterization of RE oxide nanotubes

The structure and composition of final products were characterized by scanning electron microscopy (SEM, LEO1530), transmission electron microscopy (TEM, Hitachi H600), high-resolution TEM (HRTEM, TECNAI F-30), and X-ray powder diffraction (XRD, PANalytical X-pert) using a CuKα radiation. Before TEM analysis, the AAO templates were dissolved in enough amounts of NaOH (4 M) for more than 10 h to ensure the AAO template to be totally dissolved. The final products were collected by centrifugation, and then rinsed with distilled water several times until the solution became neutral. As-prepared products were ultrasonically dispersed into ethanol solution and then dropped onto the copper grids.

3. Results and discussion

It is well known that the size and uniformity of the final one-dimensional nanostructures deeply depend on applied AAO templates. Fig. 1a shows a typical top-view SEM image of a blank AAO membrane after widened by phosphoric acid. Obviously, the pores of the AAO membrane take approximate hexagonal arrangement like a honeycomb. The size of the pores is very uniform, and the average diameter is about 80 nm and the thickness of the pore wall is about 20 nm. In addition, it can be seen from its corresponding TEM image (inset in Fig. 1a) that the channels are parallel to each other, vertical to the surface of membrane. Using Ho_2O_3 as an example, typical SEM images of RE oxide nanotubes obtained by immersing porous AAO membrane in sol solution for 2 h are shown in Fig. 1b. From the top view (Fig. 1b) of porous AAO membrane (without etching of the AAO template), almost every AAO pore is filled by a nanotube, of which most are with an open end. At the same time, many Ho_2O_3 nanotubes even slightly grow out of the surface of porous AAO membrane.

The clearer view of RE oxide nanotubes is provided by the TEM characterization of the products after dissolving AAO templates by high-concentration NaOH solution. Fig. 2 shows typical TEM images of as-prepared RE oxide nanotubes including Y_2O_3, CeO_2, Pr_2O_3, Nd_2O_3, Sm_2O_3, Eu_2O_3, Gd_2O_3, Tb_2O_3, Dy_2O_3, Ho_2O_3, Er_2O_3 and Yb_2O_3 nanotubes. The diameters of RE oxide nanotubes are uniform, basically equal to the channel diameter (about 80 nm) of the applied AAO template, and the wall thicknesses are about 5–15 nm (see also Fig. 4). The lengths of RE oxide nanotubes are several hundred nanometers, obviously shorter than the pore depth (20 μm) of the applied AAO templates. It could be due to the fact that as-prepared RE oxide nanotubes broke into short tubes during intense ultrasonic dispersion treatment. This result suggests the crystallization imperfection of as-prepared RE oxide nanotubes. Interestingly, as-prepared products consist of two types of tube-like nanostructures. Most of the products consist of bamboo-like nanotubes

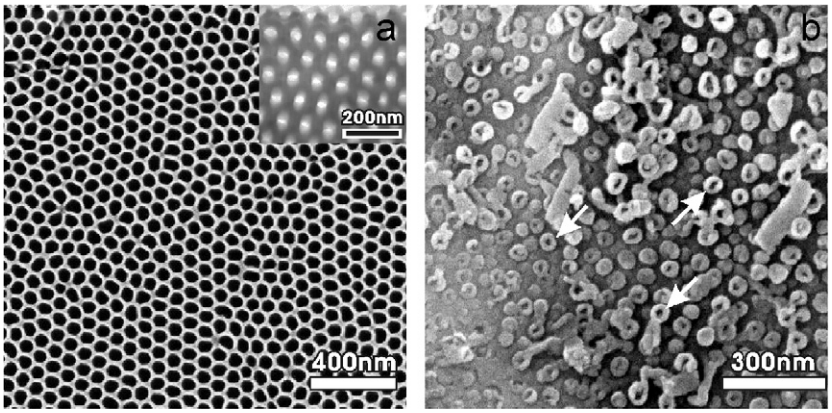

Fig. 1. (a) Typical SEM image of blank AAO membrane, the inset is its corresponding TEM image. (b) Top-view SEM image of Ho_2O_3 nanotubes grown in the AAO channels.

(Figs. 2b, d, e–g, i and j), and some products contain ordinary nanotubes with an entire hollow interior (Figs. 2c, k and l). However, it is still very difficult to fully control the two morphologies, respectively. For the bamboo-like nanotubes, their interiors are divided into many cavities separated by thin walls with the thickness of 5–10 nm (see also Fig. 4c). The heights of these separated cavities could be unequal, ranging from tens of nanometers even to several hundreds nanometers whereas in some cases, the height of these separated cavities is yet absolutely uniform. Factually, such bamboo-like structures were ever reported in some previous studies [29] and our previous study about as-prepared ThO_2 nanotubes via porous AAO template assisted sol–gel methods [27].

Fig. 3 shows the representative XRD patterns of some as-prepared RE oxide nanotubes. Comparing with standard JCPDS patterns, all diffraction peaks of every product are consistent with the corresponding cubic RE oxide phases, where no diffraction peak of impurities is found in the patterns. Due to well-known lanthanide contraction effect, the diffraction peaks of RE oxide nanotubes slightly shift to high angle with the increase of atomic number. In addition, the relatively broadened diffraction peaks reveal that as-prepared RE oxide nanotubes are composed of small nanoparticles. According to the Scherrer formula, the average diameter of the crystallites composing various RE oxide nanotubes is estimated to be in the range of 5–10 nm from (1 1 1)/(2 2 2) diffraction peaks of the patterns.

More detailed structure information about two types of RE oxide nanotubes is provided by corresponding HRTEM images. As an example, HRTEM images of as-prepared Ho_2O_3 nanotubes are shown in Fig. 4. It can be seen in Fig. 4a that the first type of Ho_2O_3 nanotubes is entirely hollow and still maintains parallel growth, and the thickness is about 5 nm. Detailed HRTEM observation (Fig. 4b) shows that local walls of Ho_2O_3 nanotubes represent a clearly resolved (2 2 2) lattice fringe with 0.30 nm spacing. It also indicates that the walls of Ho_2O_3 nanotubes consist of numerous nanoparticles of about 5–10 nm, being in good agreement with the value estimated from XRD diffraction. The corresponding SAED pattern proves the polycrystalline property of Ho_2O_3 nanotubes (inset in Fig. 4a). However, several bright diffraction spots appear in addition to the uniform diffraction rings, indicating the preferential orientation of the crystallites in the nanotubes. As the preferential growth of crystallites can be considered as single crystalline growth to some extent, it might lead to the polycrystalline nanotubes slightly growing out of the AAO template surface. The bamboo-like nanotubes as shown in Figs. 4c and d represent similar polycrystalline walls. The only difference between them is the emergence of septa in the interior of Ho_2O_3 nanotubes.

For the analyses of nanotubes or nanowires prepared in AAO template, special attention must be paid to them in order to avoid mistaking the alumina nanotubes for as-prepared nanotubes. As pointed out in the previous report, large quantity of alumina nanotubes/nanowires can be produced at room temperature when porous AAO templates are etched in an aqueous NaOH solution for appropriate time [30]. We also found that the products consisted of large amount of alumina by checking the products with energy dispersive X-ray (EDX) spectroscopy if we only etched the AAO templates for 2 h or shorter time in high-concentration NaOH solution as usually reported. This phenomenon suggests that we should at least reconsider the productivity of many reported nanowires and nanotubes by employing AAO templates. To our experience, top-view SEM observations on un-etched AAO template such as Fig. 1b are convinced. To observe an etched AAO template, one should assure all the aluminum oxide to be dissolved. A high-concentration NaOH solution (4 M) and the etching time over 10 h have been found to dissolve the AAO templates completely, as EDX elemental analyses finally showed the absence of aluminum element.

Although the sol–gel method associated with porous AAO templates is very efficient to prepare diversified monocomponent or multicomponent nanowires/nanotubes

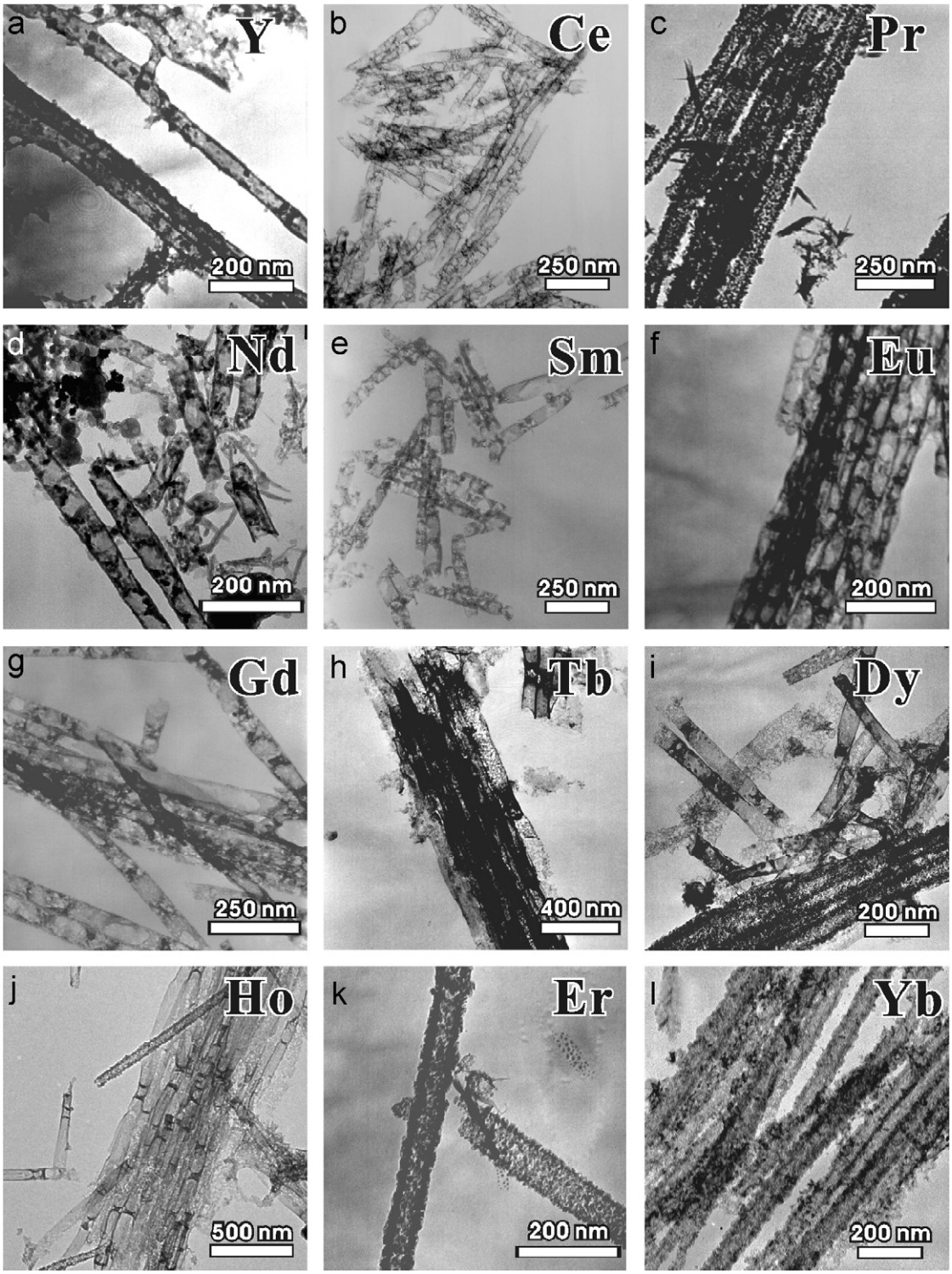

Fig. 2. Typical TEM images of RE oxides after dissolving the AAO templates with the high-concentration NaOH solution: (a) Y_2O_3; (b) CeO_2; (c) Pr_2O_3; (d) Nd_2O_3; (e) Sm_2O_3; (f) Eu_2O_3; (g) Gd_2O_3; (h) Tb_2O_3; (i) Dy_2O_3; (j) Ho_2O_3; (k) Er_2O_3; (l) Yb_2O_3.

[20–26], there are still some technique difficulties in obtaining nanowires or nanotubes at will. The main reason is that it is very complicated during the immersing and calcination procedures. It is well known that the only driving force for the sol to fill into the AAO pores is capillary action. However, the viscosity of the sols resulted from different precursors is always distinct, which inevitably affects the amount of sol to be filled in the AAO pores. During subsequent calcination treatment, the sols gradually come into being gels, and then decompose and crystallize into the corresponding RE oxide nanostructures. This process accompanies with the release of some gas.

These two steps are too complicate to be uncovered intrinsically until now. Generally, to form nanotubes, the products should homogenously nucleate and grow on the wall of AAO pores; on the other hand, the decomposed nanoparticles should congregate in the AAO pores during the calcination process to form solid nanowires. These two processes could be very difficult to be controlled accurately. Therefore, many previous studies showed a mixture of nanotubes and nanowires. Obviously, in our experimental condition, we have successfully controlled the formation of almost all RE oxide nanotubes. One main characteristic of our strategy is that we simply used RE nitrate solutions as the sol precursors, where no organic component was included. Furthermore, due to the similarity of physical and chemical properties between RE elements, the viscosity of resulting RE sols through identical synthetic process could be similar. As for the calcination treatment, we try our best to ensure identical heating rate and heating temperature in every experiment.

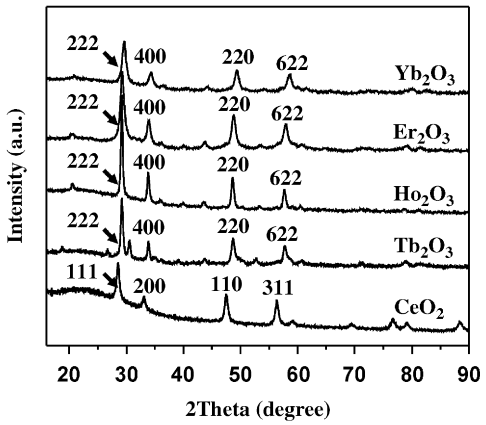

Fig. 3. XRD patterns of as-prepared RE oxide nanotubes (JCPDS: 43-1002 for CeO_2; JCPDS: 23-1418 for Tb_2O_3; JCPDS: 44-1268 for Ho_2O_3; JCPDS: 01-0827 for Er_2O_3; JCPDS: 43-1037 for Yb_2O_3).

Based on our experimental facts, we proposed a possible formation mechanism of RE oxide nanotubes as shown in Fig. 5. Firstly, the sols fully fill into AAO pores when porous AAO templates are immersed in sol. During the calcinations, the sol first changes into gel. This process may accompany the release of small amount of gases. Thus, the formation of gels is a mass loss process and the gels may form nanotubes in the AAO pore. If there exists strong interaction between the gel and AAO pore wall, the gel very possibly coats on the AAO wall homogeneously and forms gel nanotubes. Our case matched this point, as we did not use organic additives to prepare the sol and the gel should be hydrates that have strong interactions with the oxygen atoms on the AAO pore wall. Many previous reports used the organic components such as citrates to prepare the sol–gel. The organic components may weaken the interactions between the gel and the AAO wall, and

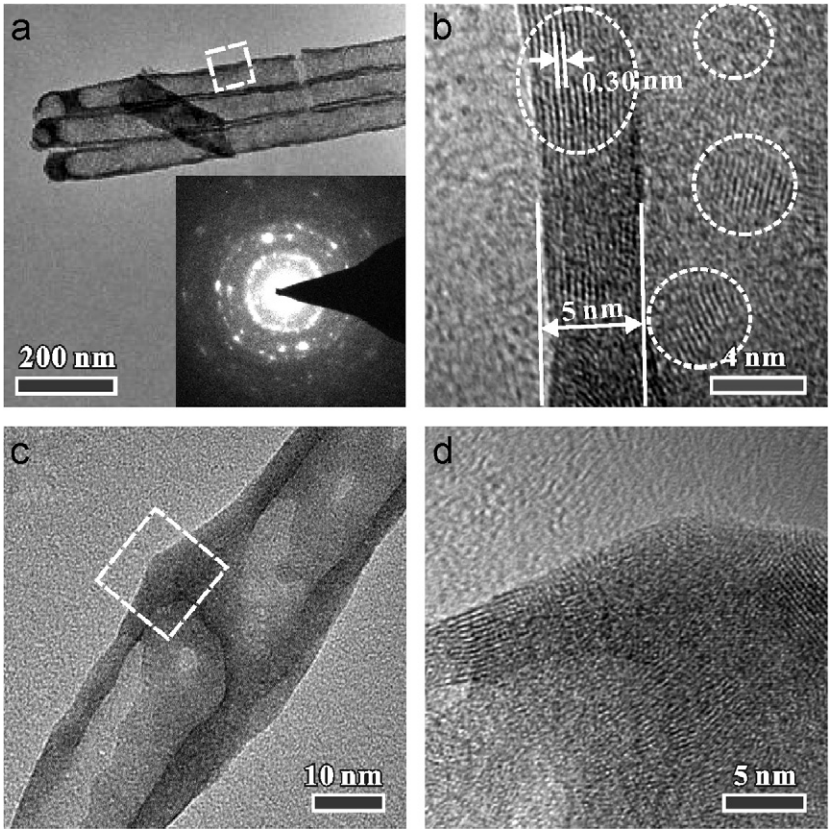

Fig. 4. Typical HRTEM images of two types of Ho_2O_3 nanotubes: (a), (b) entirely hollow nanotubes; (c), (d) bamboo-like Ho_2O_3 nanotubes; (b) and (d) are, respectively, taken from the area marked with white squares in (a) and (c). The inset in (a) is the corresponding SAED pattern of Ho_2O_3 nanotubes.

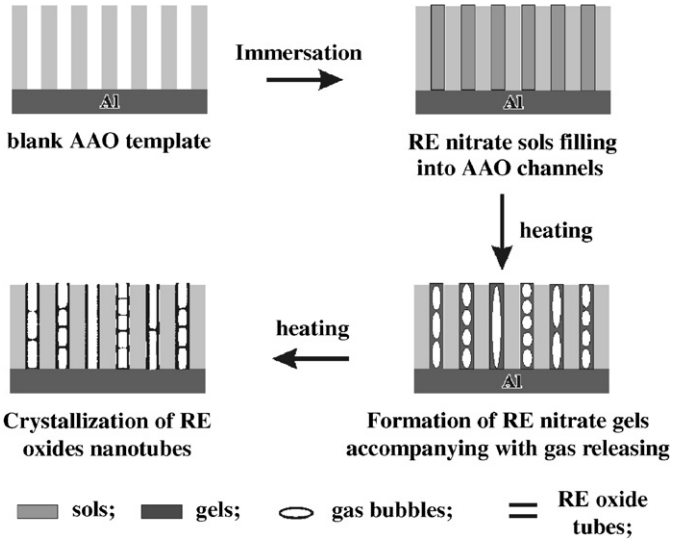

Fig. 5. Schematic of a possible formation mechanism of two types of RE oxide nanotubes.

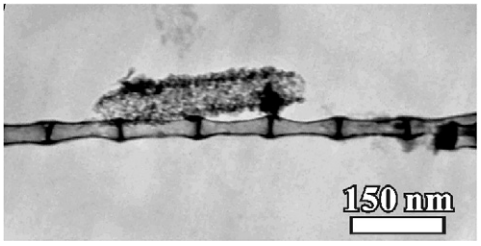

Fig. 6. Some bamboo-like Ho_2O_3 nanotubes with non-uniform diameters along the tube.

thus most of the products are nanowires or the mixture of nanowires and nanotubes.

The formation of either straight nanotubes or the bamboo-like nanotubes may depend on the viscosity of the sol. For a sol with specific viscosity, the released gas may serve as template and result in the formation of bamboo-like gel nanotubes in the AAO pores because of the tension of the gas bubble surfaces. By comparing the morphology of the as-prepared straight nanotubes and the bamboo-like nanotubes as shown in Fig. 2, it can be found that the walls of the straight nanotubes are less dense than that of bamboo-like nanotubes, which may reflect the difference of the viscosities of the sols when preparing the two kinds of nanotubes.

As for the growth of nanotubes in AAO pores, another possible mechanism is that the nucleation occurs on these active sites of AAO pore walls and then the corresponding oxide nanotubes are grown because porous AAO pore walls usually have large amounts of structural defects. However, our experimental results show that some bamboo-like nanotubes are not in uniform size along the tube as shown in Fig. 6. The septa positions are much larger than other parts. It is known that the AAO pores are usually very straight. Therefore, at least for this kind of non-uniform bamboo-like nanotubes, the nucleation and the growth of final RE oxide nanotubes need not be absolutely confined on the AAO pore walls. The result also implies that the nanotubes may have already formed during the formation of gel.

4. Summary

In this paper, we report a versatile synthetic method of RE oxide nanotubes. Arrays of RE oxide nanotubes (RE = Y, Ce, Pr, Nd, Sm, Eu, Gd, Tb, Dy, Ho, Er, Yb) were successfully prepared from corresponding RE nitrate solution via the sol–gel method assisted with porous AAO templates. Detailed TEM observation indicates that as-prepared RE oxides evolve into two types of tube-like nanotubes including bamboo-like nanotubes and entirely hollow nanotubes. The formation of gel nanotubes in the AAO channels is proposed as a new possible growth mechanism of RE oxide nanotubes.

Acknowledgments

This work is supported by the NSFC (Grant nos. 20673085, 20473069 and 20671078), the Key Scientific Project of Fujian Province of China (Grant no. 2005HZ01-3), NCET from the Ministry of Education of China and the Fok Ying-Tung Educational Foundation.

References

[1] (a) J. Mckittrick, L.E. Shea, C.F. Bacalski, E.J. Bosze, Displays 19 (1999) 169;
(b) T. Justel, H. Nikol, C. Ronda, Angew. Chem. Int. Ed. 37 (1998) 3085.
[2] (a) T.S. Chin, J. Magn. Magn. Mater. 209 (2000) 75;
(b) M. Tomota, M. Murakami, Nature 421 (2003) 517;
(c) S.J. Collocott, J.B. Dunlop, H.C. Lovatt, V.S. Ramsden, Rare Earths '98 Mater. Sci. Forum 3 (1999) 77;
(d) C. Ying, P. Chi, X.J. Yu, P. Wei, L. Wei, F.Z. Lian, J. Rare Earth 23 (2005) 263.
[3] (a) Y.Q. Shen, Z.Q. Shen, Y.F. Zhang, K.M. Yao, Macromolecules 29 (1996) 8289;
(b) Q. Miao, G.X. Xiong, S.S. Sheng, W. Cui, L. Xu, X.X. Guo, Appl. Catal. A 154 (1997) 17;
(c) F. Cavani, F. Trifiro, Catal. Today 51 (1999) 561;
(d) O.V. Buyevskaya, D. Wolf, M. Baerns, Catal. Today 62 (2000) 91;
(e) M. Schappacher, T. Fabre, A.F. Mingotaud, A. Soum, Biomaterials 22 (2001) 2849.
[4] G. Wakefield, E. Holland, P.J. Dobson, J.L. Hutchison, Adv. Mater. 13 (2001) 1557.
[5] J.A. Capobianco, F. Vetrone, J.C. Boyer, A. Speghini, M. Bettinelli, J. Phys. Chem. B 106 (2002) 1181.
[6] X.Y. Song, J.X. Zhang, M. Yue, E.D. Li, H. Zeng, N.D. Lu, M.L. Zhou, T.Y. Zuo, Adv. Mater. 18 (2006) 1210.
[7] M. Yada, M. Mihara, S. Mouri, M. Kuroki, T. Kijima, Adv. Mater. 14 (2002) 309.
[8] M. Yada, C. Taniguchi, T. Torikai, T. Watari, S. Furuta, H. Katsuki, Adv. Mater. 16 (2004) 1448.
[9] Y.P. Fang, A.W. Xu, L.P. You, R.Q. Song, J.C. Yu, H.X. Zhang, Q. Li, H.Q. Liu, Adv. Funct. Mater. 13 (2003) 955.
[10] X. Wang, Y.D. Li, Chem. Eur. J. 9 (2003) 5627.

[11] X. Wang, X.M. Sun, D.P. Yu, B.S. Zou, Y.D. Li, Adv. Mater. 15 (2003) 1442.
[12] X. Wang, Y.D. Li, Angew. Chem. Int. Ed. 42 (2003) 3497.
[13] M.H. Huang, S. Mao, H. Feick, H.Q. Yan, Y.Y. Wu, H. Kind, E. Weber, R. Russo, P.D. Yang, Science 292 (2001) 1897.
[14] Q.H. Wang, M. Yan, R.P.H. Chang, Appl. Phys. Lett. 78 (2001) 1294.
[15] (a) S.H. Jeong, H.Y. Hwang, K.H. Lee, Appl. Phys. Lett. 78 (2001) 2052;
(b) J.S. Lee, G.H. Gu, H. Kim, K.S. Jeong, J. Bae, J.S. Suh, Chem. Mater. 13 (2001) 2387;
(c) E.J. Bae, W.B. Choi, K.S. Jeong, J.U. Chu, G.S. Park, S. Song, I.K. Yoo, Adv. Mater. 14 (2002) 277;
(d) H. Chik, J. Liang, S.G. Cloutier, N. Kouklin, J.M. Xu, Appl. Phys. Lett. 84 (2003) 3376.
[16] (a) Z.A. Hu, T. Xu, R.J. Liu, H.L. Li, Mater. Sci. Eng. A 371 (2004) 236;
(b) H. Pan, H. Sun, C. Poh, Y.P. Feng, J.Y. Lin, Nanotechnology 16 (2005) 1559.
[17] (a) J.C. Bao, C.Y. Tie, Z. Xu, Q.F. Zhou, D. Shen, Q. Ma, Adv. Mater. 13 (2001) 1631;
(b) Y.K. Su, D.H. Qin, H.L. Zhang, H. Li, H.L. Li, Chem. Phys. Lett. 388 (2004) 406;
(c) G.W. Meng, A.Y. Cao, J.Y. Cheng, A. Vijayaraghavan, Y.J. Jung, M. Shima, P.M. Ajayan, J. Appl. Phys. 97 (2005) 064303;
(d) A. Saedi, M. Ghorbani, Mater. Chem. Phys. 91 (2005) 417.
[18] (a) H.Q. Cao, Y. Xu, J.M. Hong, H.B. Liu, G. Yin, B.L. Li, C.Y. Tie, Z. Xu, Adv. Mater. 13 (2001) 1393;
(b) J.X. Ding, J.A. Zapien, W.W. Chen, Y. Lifshitz, S.T. Lee, X.M. Meng, Appl. Phys. Lett. 85 (2004) 2361;
(c) C.H. Bae, S.M. Park, S.C. Park, J.S. Ha, Nanotechnology 17 (2006) 381.
[19] A.K. Raychaudhuri, K.S. Shankar, Mater. Sci. Eng. 25 (2005) 738.
[20] L.F. Cheng, X.T. Zhang, B. Liu, H.Z. Wang, Y.C. Li, Y.B. Huang, Z.L. Du, Nanotechnology 16 (2005) 1341.
[21] H. Xu, D.H. Qin, Z. Yang, H.L. Li, Mater. Chem. Phys. 80 (2003) 524.
[22] B.B. Lakshmi, P.K. Dorhout, C.R. Martin, Chem. Mater. 9 (1997) 857.
[23] Z. Miao, D.S. Xu, J.H. Ouyang, G.L. Guo, X.S. Zhao, Y.Q. Tang, Nano Lett. 2 (2002) 717.
[24] (a) Y.K. Zhou, J. Huang, C.M. Shen, H.L. Li, Mater. Sci. Eng. A 335 (2002) 260;
(b) Y.K. Zhou, C.M. Shen, J. Huang, H.L. Li, Mater. Sci. Eng. B 95 (2002) 77;
(c) Y.K. Zhou, C.M. Shen, H.L. Li, Solid State Ionics 146 (2002) 81.
[25] (a) G.B. Ji, S.L. Tang, B.L. Xu, B.X. Gu, Y.W. Du, Chem. Phys. Lett. 379 (2003) 484;
(b) Z. Yang, Y. Huang, B. Dong, H.L. Li, S.Q. Shi, Appl. Phys. A 84 (2006) 117;
(c) Y.K. Zhou, H.L. Li, J. Mater. Chem. 12 (2002) 681.
[26] (a) S.Z. Chu, K. Wada, S. Inoue, S.I. Todoroki, Chem. Mater. 14 (2002) 266;
(b) X.H. Li, W.M. Liu, H.L. Li, Appl. Phys. A 80 (2005) 317;
(c) S.X. Xiong, Q. Wang, H.S. Xia, Synth. Met. 146 (2004) 37.
[27] Z.W. Lin, Q. Kuang, W. Lian, Z.Y. Jiang, Z.X. Xie, R.B. Huang, L.S. Zheng, J. Phys. Chem. B 110 (2006) 23007.
[28] S.H. Zhang, Z.X. Xie, Z.Y. Jiang, X. Xu, J. Xiang, R.B. Huang, L.S. Zheng, Chem. Commun. (2004) 1106.
[29] T.Y. Peng, H.P. Yang, G. Chang, K. Dai, K. Hirao, Chem. Lett. 33 (2004) 336.
[30] Z.L. Xiao, C.Y. Han, U. Welp, H.H. Wang, W.K. Kwok, G.A. Willing, J.M. Hiller, R.E. Cook, D.J. Miller, G.W. Crabtree, Nano Lett. 2 (2002) 1293.